Cellular Physiology and Biochemistry

Cell Physiol Biochem 2017;44:2105-2116
DOI: 10.1159/000485949
Published online: December 12, 2017
Accepted: November 17, 2017

Original Paper

Exosomes from MiR-126-Overexpressing Adscs Are Therapeutic in Relieving Acute Myocardial Ischaemic Injury

Qiancheng Luo Dongfeng Guo Guorong Liu Guo Chen Min Hang Mingming Jin

Department of Emergency Medicine, Shanghai Gongli Hospital, Second Military Medical University, Shanghai, P.R. China

Key Words
Exosomes • ADSCs • Acute myocardial ischaemia • MiR-126 • Apoptosis

Abstract
Background/Aims: Recent studies have indicated that exosomes play an important role in adipose-derived stem cell (ADSC) transplant-mediated ischaemic heart disease therapy. However, the treatment effect is not obvious. The aim of this study is to investigate whether ADSC-derived exosomes enriched with microRNA (miR)-126 have a more protective effect on acute myocardial infarction (AMI). ***Methods:*** Exosomes were characterized by transmission electron microscopy, and the exosome particles were further examined using nanoparticle tracking analyses. A rat model of myocardial infarction and *in vitro* model of hypoxia-induced H9c2 myocardial cell injury were established to study the protective mechanism of exosomes from miR-126-overexpressing ADSCs. ***Results:*** The *in vitro* results showed that exosomes derived from miR-126-overexpressing ADSCs decreased H9c2 myocardial cell injury by reducing inflammation factor expression during hypoxia induction. The miR-126-enriched exosomes also decreased the expression of fibrosis-related proteins of H9c2 cells under hypoxic conditions. Matrigel® and Transwell® assays showed that miR-126-enriched exosomes significantly promoted microvascular generation and migration, respectively. *In vivo* studies confirmed that exosomes derived from ADSCs significantly decreased the myocardial injury area of infarction, especially after miR-126-enriched exosome treatment. Cardiac fibrosis and inflammatory cytokine expression were also decreased after treatment with miR-126-enriched exosomes. However, blood vessel formation was promoted in the infarction region of AMI rats. ***Conclusions:*** The results suggested that the expression of miR-126-enhanced ADSC-derived exosomes prevented myocardial damage by protecting myocardial cells from apoptosis, inflammation, fibrosis, and increased angiogenesis.

Q. Luo and D. Guo contributed equally to this work.

Guo Chen, Min Hang and Mingming Jin

Department of Emergency Medicine, Shanghai Gongli Hospital, Second Military Medical University, 219 Miao-Pu Road, Shanghai (China)
E-Mail guo_guo_chen@163.com, 13817577126@139.com, asdjinmingming@126.com

Introduction

Acute myocardial infarction (AMI) is a leading cause of death worldwide [1, 2]. Recent studies have found that stem cell transplantation is useful for treating myocardial infarction [3]. Many groups have used adipose-derived stem cells (ADSCs) because they are abundant, lack donor limitations, and present a low risk of side effects. After lineage-specific stimulation, ADSCs show multi-differentiation potential. Additionally, ADSCs secrete numerous cytokines and growth factors that confer reparative capabilities after stem cell mobilization or transplantation. In addition to these advantages, many studies have used ADSCs for cell therapies and tissue engineering due to their ease of obtainment and varied applications. However, transplanted ADSCs survive poorly in the inflammatory and ischaemic microenvironment of acute myocardial infarction [4, 5]. To increase the survival of the transplanted cells, genetically engineered methods have been used [6, 7], but ethical and safety challenges remain.

Therefore, further studies are necessary to improve the microenvironment of myocardial infarction and enhance the effects of stem cells under safer conditions. Exosomes (30- to 100-nm small membrane vesicles) derived from ADSCs have been used to treat AMI [7, 8]. Exosome-mediated cell-cell microcommunication through inherent molecules such as nucleotides, proteins, and bioactive lipids has been reported [9-11]. Exosomes play an important role as key transporters of paracrine factors in angiogenesis, immune regulation, and tissue regeneration [12-14]. However, the contribution of exosomes to the cardiac microenvironment after acute myocardial infarction still needs further understanding.

MicroRNAs (miRNAs) are small, endogenous, noncoding RNAs that post-transcriptionally regulate gene expression. They play a critical role in proliferation, differentiation, apoptosis, and the stress response. Recently, several reports have suggested that miRNAs suppressed the myocardial damage after AMI by improving the myocardial tissue microenvironment [15-17].

Recently, studies have shown that miR-126 plays an important role in improving myocardial damage after AMI [18, 19]. To further study this effect, we used ADSC-derived exosomes with increased levels of miR-126. The therapeutic effects of exosomes on AMI were investigated by treating the cells or AMI rats with miR-126-overexpressing ADSC-derived exosomes. The results showed that miR-126-enriched exosomes have a better therapeutic effect by reprogramming the microenvironment of acute myocardial infarction, thus promoting improved heart function after an ischaemic injury.

Materials and Methods

Reagents

Antibodies against CD29, CD90, CD45, CD105, CD34, vWF, TGF-β, α-SMA, fibronectin, collagen I, and GAPDH were purchased from Sigma-Aldrich (St. Louis, MO, USA). The miR-126 mimics were from GenePharma (Shanghai, China). Dulbecco's Modified Eagle Medium (DMEM; high glucose), serum-free endothelial basal medium, and foetal bovine serum (FBS) were from Nego (Shanghai, China). Cell lysis buffer (10×) was obtained from Cell Signaling Technology (Danvers, MA, USA). A real-time PCR (RT-PCR) kit was purchased from Toyobo (Shanghai, China). Other reagents included 4',6-diamidino-2-phenylindole (DAPI; Roche, Mannheim, Germany) and Masson's trichrome stain (Sigma-Aldrich). All pairs of real-time PCR primers were synthesized by Shenggong Biotechnology (Shanghai, China). All chemicals and reagents were of analytical grade.

Ethical statement

All animals were treated in accordance with the Guide for the Care and Use of Laboratory Animals, and all experiments were approved and performed according to the guidelines of the Ethics Committee of Pudong New Area Gongli Hospital, Shanghai, China. All surgical procedures were performed under anaesthesia, and every effort was made to minimize suffering. Rats were anaesthetized by intraperitoneal injection of pentobarbital sodium (30 mg/kg).

Preparation, culture and identification of ADSCs

The isolation and culture of ADSCs were conducted as previously described [20]. Briefly, male Sprague-Dawley rats (80–120 g) were euthanized, and adipose tissue was obtained from the inguinal depots and washed with phosphate-buffered saline (PBS) to remove any residual blood. The tissues were cut into 1 × 1 mm sized pieces and digested with collagenase I. After centrifugation at 4, 000 g for 5 min, the cell pellet was resuspended in DMEM containing 10% FBS/1% penicillin-streptomycin/2 mM L-glutamine and was incubated in a humidified atmosphere with 5% CO_2 at 37 °C for 48 h. The medium containing non-adherent cells was then removed, and fresh culture medium was added. The medium was changed every 3 days. Cells were passaged when they were approximately 90% confluent and were used at passage three. To confirm the identity of the cells, we incubated ADSCs with conjugated monoclonal antibodies against CD29, CD90, CD45, CD105, or CD34. Isotype-identical antibodies served as controls (Pharmingen, San Diego, CA, USA). For the analyses of CD29, CD90, CD45, CD105, and CD34, cells were further incubated with a biotinylated horse anti-mouse IgG (H1L) antibody and FITC-conjugated streptavidin (Caltag, South San Francisco, CA, USA). After treatment, the cells were fixed in 1% paraformaldehyde. Quantitative analyses were performed using a FACSCalibur™ flow cytometer (BD Biosciences, San Jose, CA, USA) and FlowJo software (FlowJo, Ashland, OR, USA). The logarithmic fluorescence intensities were recorded for 10, 000–20, 000 cells per sample.

Isolation and identification of microvesicles (MVs) from conditioned medium

Culture media from both ADSC cells and miR-126-overexpressing ADSCs cells (miR-126-ADSCs) (miR-126 mimics or miR-126 NC (GenePharma, China) were transfected into ADSCs cells using Lipofectamine 2000 (Invitrogen, CA, USA) according to the manufacturer's instructions. At 48 h after transfection, cells were harvested for RT-PCR analyses) were collected and centrifuged at 3000 × *g* for 15 min to remove cells and cell debris. The supernatant was further concentrated by centrifugation for 30 min at 5000 × *g* in a pre-rinsed centrifugal filter device (Amicon Ultra-15; Millipore, Billerica, MA, USA). The samples were further mixed with ExoQuick-TC™ reagent (System Biosciences, Palo Alto, CA, USA) by vortexing, further incubated overnight, and then centrifuged at 1, 500 × *g* for 30 min at 4 °C to obtain the pellet. The pellet was resuspended in PBS. To determine the sizes of the purified vesicles, nanoparticle tracking analysis (NTA) on a NanoSight LM10 (Malvern Instruments Ltd, Malvern, UK) was performed and analysed using NTA 3.0 software (Malvern).

The protein levels of CD63, CD9, and TSG101 (representative markers of exosomes) were detected by western blotting. The concentration of the exosome proteins was assessed using the Bicinchoninic Acid Assay Kit (Beyotime, Suzhou, China). The ultrastructure of the exosomes was analysed using the Libra 120 transmission electron microscope (Zeiss, Oberkochen, Germany)

Exosome labelling and uptake

The Dil fluorescent labelling kit (Sigma-Aldrich) was used for exosome labelling. Dil (400 μL) was added to the exosome suspension and incubated for 5 min at room temperature. The reaction was then stopped by adding an equal volume of exosome-depleted bovine serum albumin, and the exosomes were washed twice with PBS to remove any unbound dye. Subsequently, the Dil-labelled or denatured exosomes were incubated with ADSCs for 24 h. The cells were then fixed and stained with DAPI, and the images were obtained using a confocal microscope.

Protective effect of ADSC exosomes on myocardia under hypoxic conditions

The cardiomyoblast cell line H9c2 was purchased from the American Type Culture Collection (ATCC, Manassas, VA, USA) and cultured in DMEM supplemented with 10% FBS. To identify the protective effect of exosomes secreted from ADSCs on myocardial, co-culturing of ADSCs and H9c2 was performed using the Transwell® system with a 0.4-μm porous membrane (Costar, Corning, NY, USA) to prevent direct cell contact. The H9c2 cells were cultured in the lower wells and grown for an appropriate period. The ADSCs were then placed in the upper wells. To mimic hypoxia injury *in vitro*, cells were cultured in a hypoxia incubator chamber (93% N_2, 2% O_2 and 5% CO_2) for 24 h. To analyse the effects of the exosomes secreted from ADSCs on hypoxic-induced H9c2 cell damage, GW4869 (Sigma-Aldrich) was added to the cultures at a concentration of 2.5 μM for 8 h to reduce the release of exosomes from ADSCs before co-culturing. Next, the H9c2 cells were harvested for biological analyses.

CCK-8 assay

Cell proliferation was assessed by a Cell Counting Kit-8 assay (CCK-8, Dojindo Molecular Technologies, Gaithersburg, MD, USA). Briefly, cells (5×10^3 cells/well) were seeded in 96-well plates. Forty-eight hours after transfection, the CCK-8 reagents were added into each well at a final concentration of 10%, and the cells were maintained at 37 °C for 1 h. The absorbance was measured at 450 nm using a Microplate Reader (Bio-Rad, Hercules, CA, USA).

Matrigel® angiogenesis assay

To determine whether ADSC exosomes promoted the angiogenesis of endothelial progenitor cells (EPCs) during hypoxic injury, we designated four experimental groups as follows: Normoxia group, EPCs were cultured in DMEM containing 10% FBS at 37 °C in humidified air with 5% CO_2; Hypoxia group, EPCs were cultured in H-DMEM containing 0.2% FBS at 37 °C in humidified air with 5% CO_2, 2% O_2, and 93% N_2; Hypoxia + exosomes group and Hypoxia + miR-126-exosomes group, H9C2 cells were cultured under the same conditions, and the ADSC exosomes were added at 200 μg/mL. Twelve hours later, the images were obtained using a microscope converted to black and white, and the images were analysed using AngioQuant software (Angioquant Freeware; www.cs.tut.fi/sgn/csb/angioquant). The tube length increase (relative to basal medium) was regarded as a measure of angiogenesis.

Transwell® migration assays

Transwell® migration assays were performed using EPC cells treated with exosomes derived from ADSCs with miR-126 overexpression. Cell migration was monitored by time-lapse imaging. The Transwell® migration assays were performed using Transwell® membranes (8 μm pore size, 6.5 mm diameter) from Corning Life Sciences (Corning, NY, USA). The bottom chambers of the Transwell® plates were filled with migration-inducing medium containing 10% FBS. The top chambers were seeded with 1×10^5 EPC cells pretreated with exosomes for 24 h. After 16 h, the cells migrated though pores to the bottom surface of the Transwell® chambers and were then fixed with 10% formaldehyde, stained with 0.5% Crystal Violet, and counted using an Olympus inverted microscope. Ten randomly selected microscopic fields were counted for each group. All experiments were performed under hypoxia conditions. The controls used normoxic conditions.

Myocardial infarction model

Male Sprague-Dawley rats weighing 220–250 g were used for myocardial infarction studies. Myocardial infarction was produced by surgical ligation of the left anterior descending coronary artery (LAD). After being anaesthetized by intraperitoneal injection of sodium pentobarbital (30 mg/kg), the chest was opened at the left fourth intercostal space, and the LAD was ligated by a 6-0 silk suture 1 mm below the tip of the left atrial appendage. Successful ligation was verified by a colour change. To analyse the effects of exosomes from ADSCs or miR-126-overexpressing ADSCs on myocardial tissue, we administered exosomes (400 μg of protein) from different groups suspended in 200 μL PBS by tail intravenous injection immediately after the ligation operation. Animals were then followed for one additional month and then euthanized. Cardiac muscle tissues were collected for histochemical analyses.

Immunohistochemical analysis

To measure apoptosis, we fixed and labelled cardiomyocytes or myocardial tissues by terminal deoxynucleotidyl transferase-mediated dUTP-biotin nick end labelling (TUNEL) using a commercially available kit (In Situ Cell Death Detection Kit; Roche Diagnostics) to label the apoptotic cell nuclei. To identify myocardial tissue fibrosis and damage, we stained myocardial tissues with Masson's trichrome. The microvessel density of the infarction regions was measured by von Willebrand Factor (vWF) staining.

Western blotting

Total proteins from cells or myocardial tissues were extracted and quantified. Next, 30–50 μg of protein of each sample was separated using 10% SDS-PAGE (stacking gel, 50 V; separating gel, 100 V) and was transferred to nitrocellulose membranes (100 V, 75 min). The membranes were then blocked and incubated with primary antibodies followed by secondary antibodies. Horseradish peroxidase-labelled secondary antibodies were detected using chemiluminescence, and the greyscale image of the protein bands was analysed using Gel-pro Image Analysis Software (Media Cybernetics, Rockville, MD, USA).

RT-PCR analysis

Total RNA was isolated using a mirVana RNA Isolation Kit (Ambion, Naugatuck, CT, USA). The miR-126 and U6 levels were determined using TaqMan® MicroRNA Assays (Ambion, Invitrogen Life Technologies, Waltham, MA, USA) by RT-PCR amplification in a MyiQ Single-Colour Real-Time PCR Detection System (Bio-Rad). Cycle threshold (Ct) values were extracted, and ΔΔCt values were calculated to determine relative abundances.

Statistical analysis

The data are expressed as the means ± standard deviation (SD) from at least three independent experiments and were analysed using one-way ANOVA and Tukey's post hoc test. In all cases, $P < 0.05$ was considered statistically significant.

Results

Characterization of ADSCs and exosomes

Isolated ADSCs were labelled with different cell surface markers to determine the cell phenotypes. ADSCs were positive for the MSC markers CD29, CD90, CD44, and CD105 and negative for the endothelial markers CD34 and vWF, as previously reported (Fig. 1) [20].

The exosomes purified from ADSCs using the ExoQuick-TC™ reagent were 50–100

nm in diameter, as determined by transmission electron microscopy (Fig. 2a). Most exosomes were membrane vesicles. CD63, a representative marker of exosomes, was detected by flow cytometry (Fig. 2b). These data demonstrated that ADSC-derived exosomes were successfully purified. To further investigate the size distribution profile of the ADSC-derived exosomes, we performed size analyses using the nanoparticle tracking system, revealing a peak size of 83.8 nm (Fig. 2b). The expression of the exosome markers CD9, CD63, and TSG101 were then confirmed by western blotting (Fig. 2c).

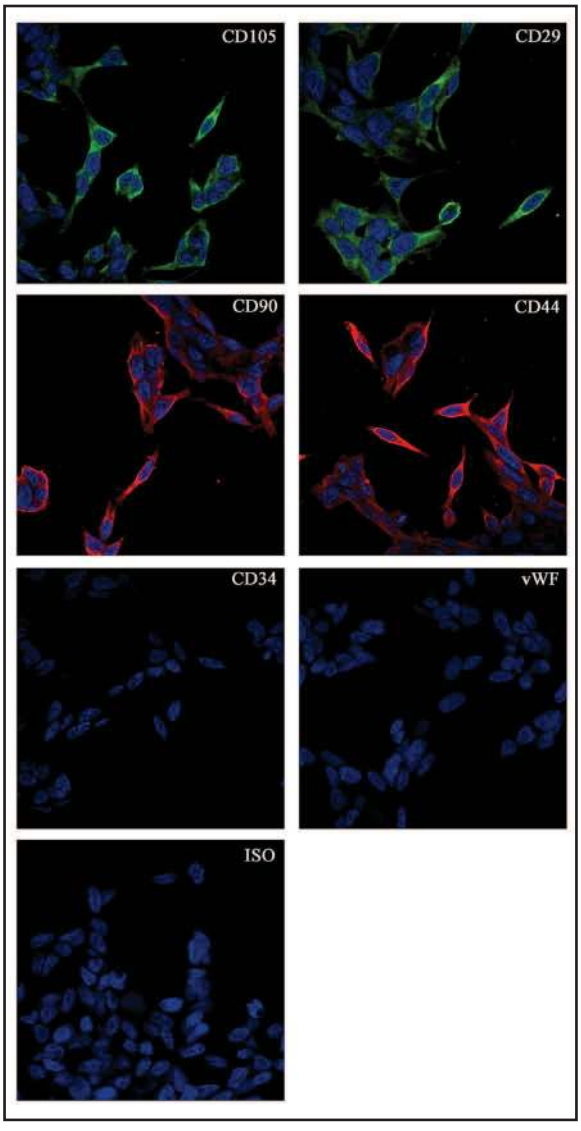

Fig. 1. Characteristics of adipose-derived stem cells (ADSCs). Determination of cell surface markers with immunofluorescence staining. The antibodies were labelled with either fluorescein isothiocyanate (FITC; green colour) or phycoerythrin (PE; red colour), respectively. CD29, CD90, CD44, and CD105 were stained positive. CD34 and von Willebrand Factor (vWF) staining were negative. Negative FITC and PE-labelled mouse IgG isotype controls are shown (magnification, ×200).

Exosomes derived from miR-126-overexpressing ADSCs have better protective effects against hypoxia-induced myocardial cell injury

RT-PCR analysis showed that after transfection with miR-126 mimics for 48 h, the expression of miR-126 in exosomes derived from ADSCs was increased compared with that in the

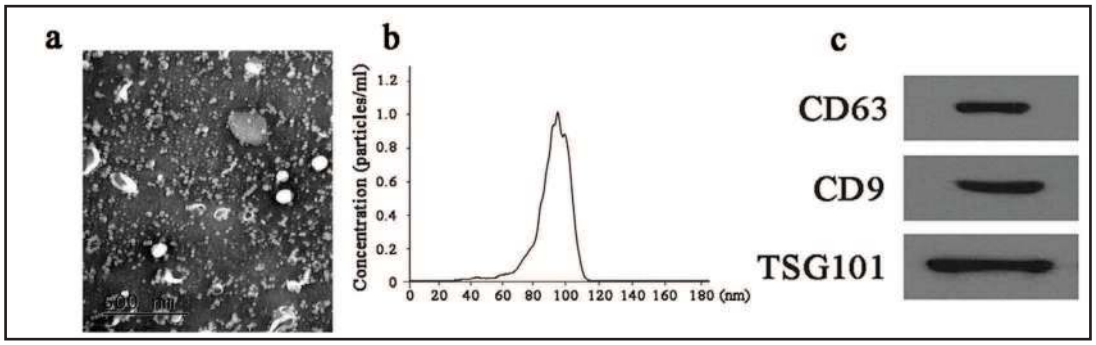

Fig. 2. Exosome characterization. (A) Electron microscopic image of exosomes. (B) Results of nanoparticle tracking analysis of exosomes. (C) Western blots using TSG101, CD9, and CD63 as markers in exosomes from ADSCs. Abbreviations are the same as those defined in the above Fig. legends.

control group (Fig. 3a). To determine whether exosomes could be transferred in a paracrine manner, we employed a Transwell® coculture system for ADSCs and H9c2 cells in which the cells were separated by a porous membrane with 0.22-μm sized pores to prevent direct cell contact or the transfer of larger vesicles (Fig. 3b). ADSC cells were transfected with pCT-CD63-GFP, a CD63-GFP fusion gene. We observed green fluorescent protein (GFP) fluorescence present in untreated H9c2 cells after 12 h of coculture, and the fluorescence intensity was more obvious after 24 h of coculture (Fig. 3c). These results showed that exosomes could be transferred between ADSCs and H9c2 cells during coculture.

To verify whether exosomes from miR-126-overexpressing ADSCs could have better protective effects against hypoxia-induced myocardial cell injury, we measured the cell viability of H9c2 cells using a CCK8 kit after coculture with ADSCs under hypoxic conditions for 24 h with or without pretreatment with GW4869 (2.5 μM). The results showed that the cell viability of H9c2 cells was suppressed after hypoxia treatment. Coculture increased the cell viability, especially coculture with miR-126-overexpressing ADSCs. However, the protective effects were decreased after pretreatment with the exosome inhibitor GW4869. The results suggested that the protective effects of ADSCs against hypoxia-induced myocardial cell injury were mediated by exosomes (Fig. 3d).

The flow cytometry results showed that the number of apoptotic cells was significantly lower in the miR-126-overexpressing ADSC-treated H9c2 cells under hypoxic conditions than in the ADSC-treated H9c2 cells. Inhibition of exosome release decreased the protective effect of ADSCs on H9c2 cells with hypoxia induction (Fig. 3e and f).

The expression levels of inflammatory factors IL-1β, IL-6, and TNF-α from H9c2 cells were detected by ELISA. The results showed that exosome release from miR-126-overexpressing ADSCs significantly decreased inflammatory factor expression and was greater than the effect with ADSC exosomes. The inhibition of exosome release from ADSCs with GW4869 pretreatment significantly prevented the protective effect of ADSCs on H9c2 cells after exposure to hypoxia (Fig. 3g–3i). Similar results were also observed for fibrosis-related protein expression as determined by western blot analyses (Fig. 3j–3n).

Exosomes derived from miR-126-overexpressing ADSCs promote the migration and angiogenesis of EPCs

Myocardial repair and the improvement of cardiac systolic function may be related to the promotion of angiogenesis. *In vitro* studies have shown that tube-like structures are significantly elevated in ADSC exosome-treated EPCs compared with that in control EPCs ($P < 0.05$). Exosomes derived from the miR-126-overexpressing ADSCs had better promoting effects than those from the other cell groups under hypoxic conditions (Fig. 4a and 4b). Moreover, the migration of EPCs in the ADSC exosome-treated group was significantly greater than that in the PBS-treated group ($P < 0.05$) after incubation under hypoxic conditions for 16 h before pretreatment with the exosomes for 24 h. The results also showed that exosomes

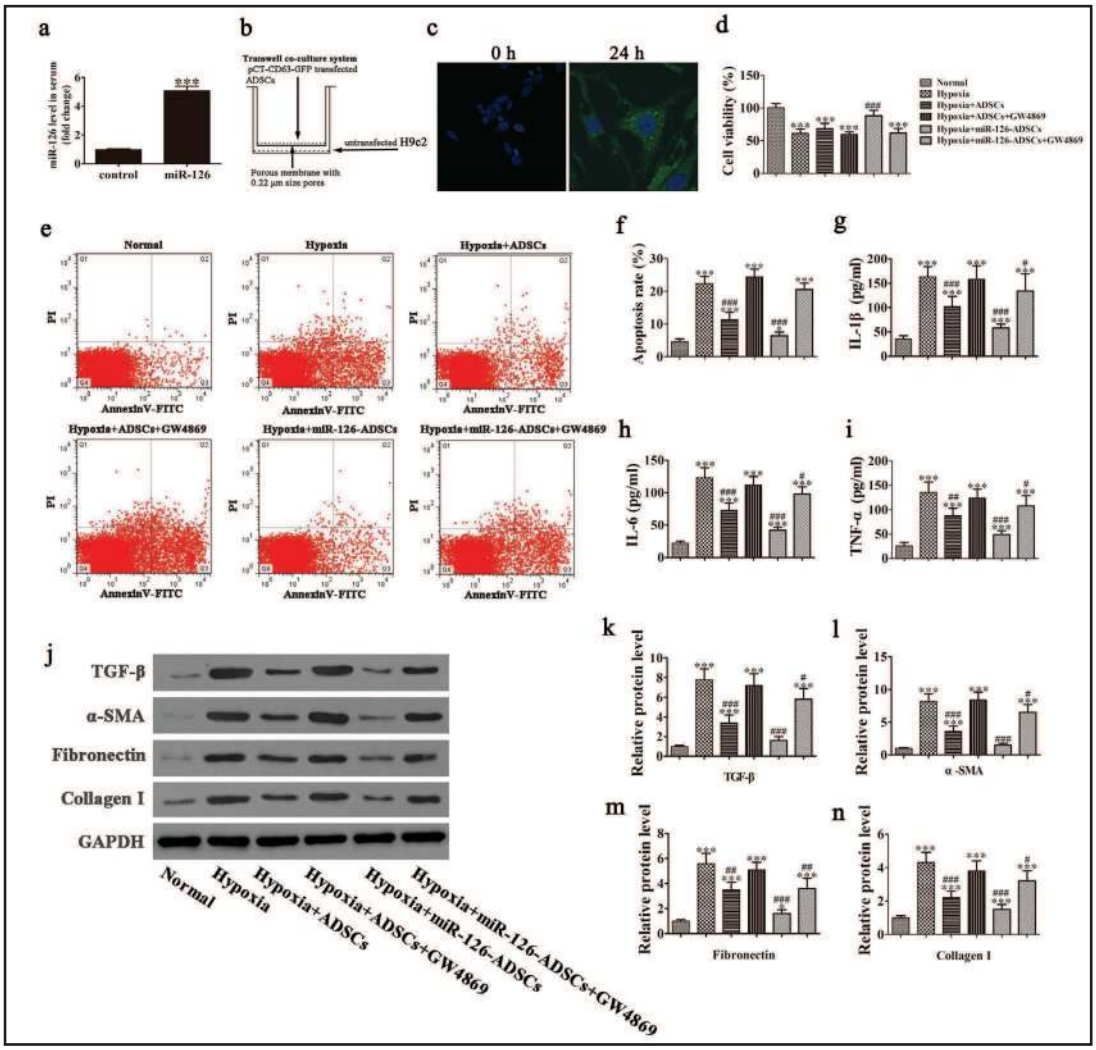

Fig. 3. Protective effect of exosomes derived from adipose-derived stem cells (ADSCs) and miR-126-overexpressing ADSCs during hypoxia-induced myocardial cell injury. (A) RT-PCR shows the expression of miR-126 in the exosomes of ADSCs after transfection with miR-126 mimics for 48 h. The data are presented as means ± SD. N = 5. ***P<0.001 vs. control. (B) A Transwell® coculture assay system was used with pCT-CD63-GFP-transfected ADSCs seeded in the top compartment, which was separated by a porous 0.22-μm membrane from the non-transfected H9c2 cells cultured in the bottom compartment. (C) Green fluorescent protein (GFP) expression in non-transfected H9c2 cells was observed by confocal microscopy (×400) after coculture for 0 h or 24 h. (D) The relative cell viability of H9c2 cells was detected using a CCK8 assay after coculture with ADSCs under hypoxic conditions for 24 h with or without pretreatment with GW4869. The data are presented as the means ± SD. N = 5. *P<0.05, ***P<0.001 vs. normal group. $^{###}$P<0.001 vs. hypoxia group. (E) Apoptosis of H9c2 cells was assessed using flow cytometry with annexin V-FITC staining. (F) The relative apoptosis ratio was analysed at least five times. The data are presented as the means ± S.D. N = 5. ***P<0.001 vs. normal group. $^{###}$P<0.001 vs. hypoxia group. (G–I) Inflammatory cytokine levels of IL-1β, IL-6, and TNF-α in each group from cell supernatants were measured. The data are presented as the means ± S.D. N = 5. *P<0.05, ***P<0.001 vs. normal group. $^{#}$P<0.05, $^{##}$P<0.01, $^{###}$P<0.001 vs. hypoxia group. (J–N) Western blots showing the expression levels of TGF-β, α-SMA, fibronectin, and collagen I. Bar graphs represent quantitative differences in the expression of TGF-β, α-SMA, fibronectin, and collagen I protein between the treatment groups. The data are presented as the means ± S.D. N = 5. *P<0.05, ***P<0.001 vs. normal group. $^{#}$P<0.05, $^{##}$P<0.01, $^{###}$P<0.001 vs. hypoxia group.

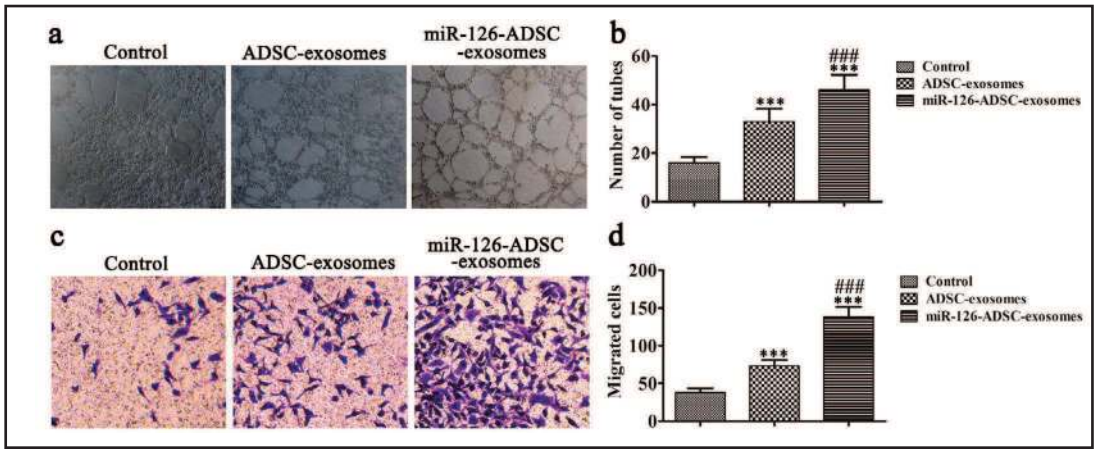

Fig. 4. ADSC exosomes accelerated tube-like structure formation and migration of endothelial progenitor cells (EPCs) after culturing with exosomes from ADSCs or miR-126-overexpressing ADSCs for 12 h under hypoxic conditions. The blood vessel capacity and migration were measured by Matrigel® and Transwell® assays, respectively. (A and B) Representative photomicrographs of tube-like structures and quantification of the tube number. The data are presented as the means ± S.D. N = 10. ***P<0.001 vs. control group. $^{###}$P<0.001 vs. exosome treatment group. (C and D) Representative photomicrographs of EPCs that migrated through the filter. The EPCs were stained with crystal violet. Quantification of cells migrating through the Transwell® membrane. The data are presented as the means ± S.D. N = 10. ***P<0.001 vs. control group. $^{###}$P<0.001 vs. exosome treatment group. Abbreviations are the same as those defined in the above Fig. legends.

derived from miR-126-overexpressing ADSCs had a greater effect on EPC migration (Fig. 4c and 4d).

Exosomes derived from miR-126-overexpressing ADSCs reduce cardiac fibrosis, suppress cell apoptosis, decrease inflammatory cytokine expression, and promote angiogenesis

Masson's trichrome staining showed that no blue-stained areas were visible in the sham group, while the percentage of cardiac fibrosis in the exosome-treated group was significantly lower than that in the PBS control group. Exosome treatment also promoted cell proliferation in the border zone, especially after treatment with exosomes from the miR-126-overexpressing ADSCs (Fig. 5a and 5b). Cardiac repair is closely associated with a reduction in cardiomyocyte apoptosis. TUNEL staining showed fewer apoptotic cells in the myocardium of the exosome-treated group than in that of the PBS-treated group. The apoptotic percentages were not significantly different between the miR-126-exosome and normal groups (Fig. 5c and 5d). To quantify angiogenesis after exosome treatment, we detected vWF-positive cells from the border zone of infarcted left ventricles by immunofluorescence staining. The results showed that vWF-positive cells in exosome-treated animals were significantly increased compared with those in the PBS-treated group, and miR-126-exosome treatment showed a better therapeutic effect than that in the other groups (Fig. 5e and 5f).

The expression levels of inflammatory factors in rat serum were detected by ELISA. The results showed that the expression levels of IL-1β, IL-6, and TNF-α were increased after AMI. The results were consistent with those of a previous study [21]. Exosome treatment significantly decreased the secretion of inflammatory factors IL-1β, IL-6, and TNF-α. Exosomes from the miR-126-overexpressing ADSCs exhibited a greater protective effect on the suppression of inflammatory factor secretion (Fig. 5g–i).

Discussion

In this study, we successfully isolated and characterized exosomes from ADSCs. The exosomes containing miR-126 displayed a greater protective effect against hypoxia-induced myocardial cell injury. In addition, miR-12-exosomes promoted the angiogenesis and

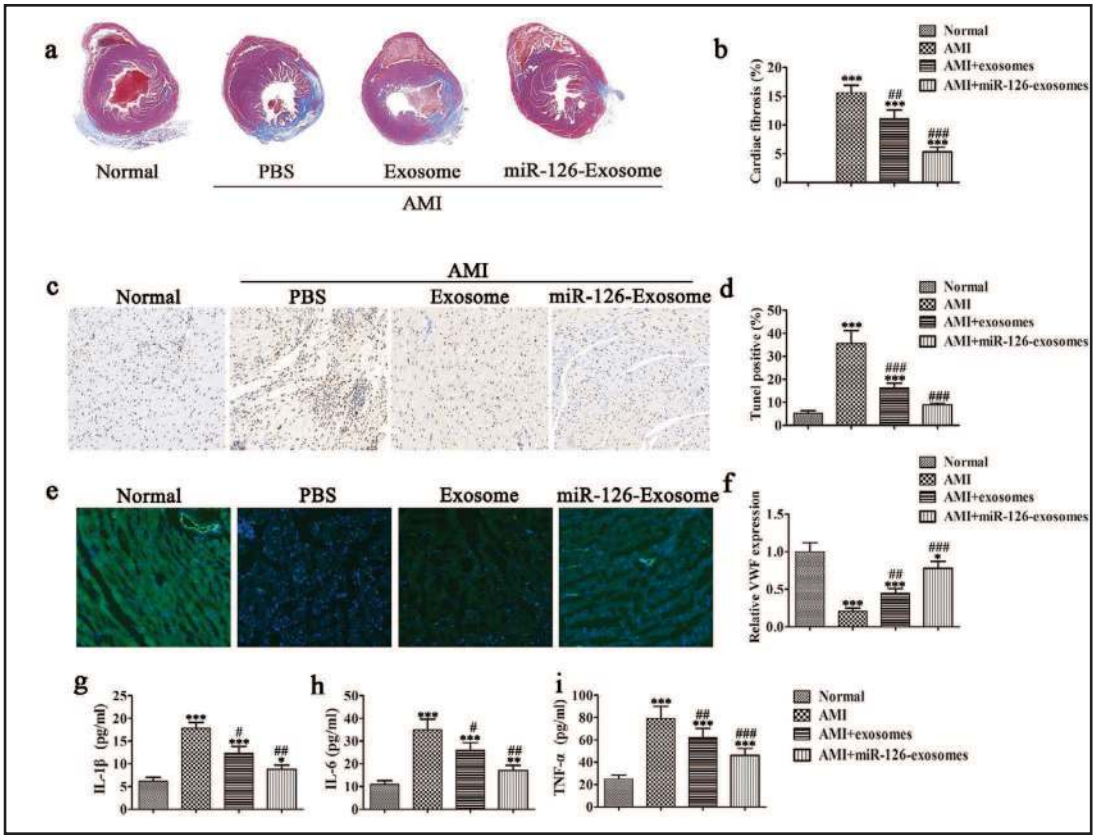

Fig. 5. Exosomes from miR-126-overexpressing ADSCs displayed a greater protective effect for reduced myocardial injury after acute myocardial infarction (AMI). (A) Micrographs show the infract size using Masson's trichrome staining in various groups 4 weeks post-infarction. Blue staining represents the infarction part of the myocardial fibrosis tissue. Red staining represents the normal myocardial tissues. (B) Quantification of the infarct size in various groups. The data are presented as the means ± S.D. N = 6. ***P<0.001 vs. normal group. $^{\#\#}$P<0.01, $^{\#\#\#}$P<0.001 vs. AMI group. (C) The myocardial apoptosis of infarction areas was measured by TUNEL staining. (D) The relative apoptosis percentages were calculated. Quantification of the infarct size in various groups. The data are presented as the means ± S.D. N = 6). ***P<0.001 vs. normal group. $^{\#\#\#}$P<0.001 vs. AMI group. (E) Immunofluorescent staining shows the density of microvessels in the infarction regions by von Willebrand Factor (vWF) staining. (F) The relative vWF staining was quantified. The data are presented as the means ± S.D. N = 6. *P<0.05, ***P<0.001 vs. normal group. $^{\#\#}$P<0.01, $^{\#\#\#}$P<0.001 vs. AMI group. (G–I) Inflammatory cytokine levels of IL-1β, IL-6, and TNF-α in serum from each group were measured by ELISA. The data are presented as the means ± S.D. N = 6. The data are presented as the means ± S.D. N = 6. *P<0.05, **P<0.01, ***P<0.001 vs. normal group. $^{\#}$P<0.05, $^{\#\#}$P<0.01, $^{\#\#\#}$P<0.001 vs. AMI group. Abbreviations are the same as those defined in the above Fig. legends.

migration of EPCs under hypoxic conditions, further suggesting that miR-126-containing exosomes have potential therapeutic effects for AMI treatment. The administration of ADSC exosomes following AMI significantly decreased cardiac fibrosis and apoptosis in an *in vivo* rat model. Exosomes from miR-126-overexpressing ADSC prevented cardiomyocyte apoptosis and promoted cell proliferation in the border zone. Furthermore, the exosomes promoted myocardial repair, which was also related to the promotion of angiogenesis and decreased inflammatory cytokine expression.

It is well known that the exosome contains mRNA, DNA, miRNAs, and proteins. The proteins and/or miRNAs carried by ADSC exosomes may be associated with the promotion of cell protection and angiogenesis. It has been reported that exosomes from ADSCs have therapeutic effects in many diseases, including AMI [22-27].

miR-126 is expressed in vascular endothelial cells and vascular smooth muscle cells and plays an important role in the process of angiogenesis through the regulation of cell proliferation, differentiation, and apoptosis [28-30]. Studies have found that the expression of circulating miR-126 was decreased after AMI [18, 19, 31]. The studies further suggested that the expression of miR-126 was enriched in endothelial cells and EPCs. miR-126 is considered a master regulator of physiological angiogenesis. The expression of miR-126 can directly target Spred1 and PI3KR2 and enhance the VEGF signalling pathway. When miR-l26 is down-regulated, the overexpression of Spred1 and PI3KR2 inhibits the MAPK and PI3K signalling pathway, which affects angiogenic factor signals and results in the disruption of angiogenesis [32, 33]. The expression of miR-126 not only can promote angiogenesis but also has anti-inflammatory effects [34, 35]. Hu J *et al.* have shown that the expression of miR-126 can significantly decrease inflammatory factor expression in a stressed environment by directly targeting SPRED1, PIK3R2, and VCAM1 through binding to their 3' untranslated region (3'-UTR) [36]. Our study also showed that miR-126 expression promoted the therapeutic effects of exosomes from ADSCs on AMI by inhibiting the tissue fibrosis of myocardial infarction areas. However, the specific action mechanism needs to be further clarified.

Stem cell transplantation has therapeutic effects on AMI [37, 38]. However, due to changes in the myocardial tissue environment after ischaemia, the function of the transplanted cells is restricted. Studies have shown that the pretreatment of transplantation cells, by processing or genetically modifying the implanted mesenchymal stem cells, will promote the therapeutic effects [39, 40]. However, some processing procedures have potential security and ethical problems. Therefore, many studies use exosomes from implanted mesenchymal stem cells. Further studies have shown that exosomes act as information vehicles, altering the behaviour of recipient cells after stem cell transplantation therapy to modulate intercellular communications. Interestingly, exosomes enriched with miRNA showed a similar therapeutic effect as ADSCs [41].

Conclusion

In summary, the results demonstrated that exosomes from autologous ADSCs may provide a promising and safe treatment strategy for AMI therapy. When transfected with miR-126, the ADSCs had increased therapeutic effects.

Disclosure Statement

The authors declare that there are no conflicts of interest regarding the publication of this paper.

Acknowledgements

This study was supported by the Shanghai Pu dong New Area Science and Technology Development Fund Innovative Funding (Health) Program (PKJ2015-Y55) and Shanghai Municipal Health and Family Planning Commission Research Project (201640405).

References

1 Plakht Y, Shiyovich A, Gilutz H: Predictors of long-term (10-year) mortality postmyocardial infarction: Age-related differences. Soroka acute myocardial infarction (sami) project. J Cardiol 2015;65:216-223.
2 Khan JN, McCann GP: Cardiovascular magnetic resonance imaging assessment of outcomes in acute myocardial infarction. World J Cardiol 2017;9:109-133.
3 Teng X, Chen L, Chen W, Yang J, Yang Z, Shen Z: Mesenchymal stem cell-derived exosomes improve the microenvironment of infarcted myocardium contributing to angiogenesis and anti-inflammation. Cell Physiol Biochem 2015;37:2415-2424.

4 Kim JH, Joo HJ, Kim M, Choi SC, Lee JI, Hong SJ, Lim DS: Transplantation of adipose-derived stem cell sheet attenuates adverse cardiac remodeling in acute myocardial infarction. Tissue Eng Part A 2017;23:1-11.
5 Lee HW, Lee HC, Park JH, Kim BW, Ahn J, Kim JH, Park JS, Oh JH, Choi JH, Cha KS, Hong TJ, Park TS, Kim SP, Song S, Kim JY, Park MH, Jung JS: Effects of intracoronary administration of autologous adipose tissue-derived stem cells on acute myocardial infarction in a porcine model. Yonsei Med J 2015;56:1522-1529.
6 Shi CZ, Zhang XP, Lv ZW, Zhang HL, Xu JZ, Yin ZF, Yan YQ, Wang CQ: Adipose tissue-derived stem cells embedded with enos restore cardiac function in acute myocardial infarction model. Int J Cardiol 2012;154:2-8.
7 Zhu XY, Zhang XZ, Xu L, Zhong XY, Ding Q, Chen YX: Transplantation of adipose-derived stem cells overexpressing hhgf into cardiac tissue. Biochem Biophys Res Commun 2009;379:1084-1090.
8 Zhang Y, Yu M, Tian W: Physiological and pathological impact of exosomes of adipose tissue. Cell Prolif 2016;49:3-13.
9 Camussi G, Deregibus MC, Bruno S, Cantaluppi V, Biancone L: Exosomes/microvesicles as a mechanism of cell-to-cell communication. Kidney Int 2010;78:838-848.
10 Tan M, Yan HB, Li JN, Li WK, Fu YY, Chen W, Zhou Z: Thrombin stimulated platelet-derived exosomes inhibit platelet-derived growth factor receptor-beta expression in vascular smooth muscle cells. Cell Physiol Biochem 2016;38:2348-2365.
11 Li J, Yu J, Zhang H, Wang B, Guo H, Bai J, Wang J, Dong Y, Zhao Y, Wang Y: Exosomes-derived mir-302b suppresses lung cancer cell proliferation and migration via tgfbetarii inhibition. Cell Physiol Biochem 2016;38:1715-1726.
12 Lai RC, Arslan F, Lee MM, Sze NS, Choo A, Chen TS, Salto-Tellez M, Timmers L, Lee CN, El Oakley RM, Pasterkamp G, de Kleijn DP, Lim SK: Exosome secreted by msc reduces myocardial ischemia/reperfusion injury. Stem Cell Res 2010;4:214-222.
13 Jia R, Li J, Rui C, Ji H, Ding H, Lu Y, De W, Sun L: Comparative proteomic profile of the human umbilical cord blood exosomes between normal and preeclampsia pregnancies with high-resolution mass spectrometry. Cell Physiol Biochem 2015;36:2299-2306.
14 Zhang J, Zhang HD, Yao YF, Zhong SL, Zhao JH, Tang JH: Beta-elemene reverses chemoresistance of breast cancer cells by reducing resistance transmission via exosomes. Cell Physiol Biochem 2015;36:2274-2286.
15 Guo ML, Guo LL, Weng YQ: Implication of peripheral blood mirna-124 in predicting acute myocardial infarction. Eur Rev Med Pharmacol Sci 2017;21:1054-1059.
16 Yuan M, Zhang L, You F, Zhou J, Ma Y, Yang F, Tao L: Mir-145-5p regulates hypoxia-induced inflammatory response and apoptosis in cardiomyocytes by targeting cd40. Mol Cell Biochem 2017;431:123-131.
17 Yang J, Brown ME, Zhang H, Martinez M, Zhao Z, Bhutani S, Yin S, Trac D, Xi JJ, Davis ME: High-throughput screening identifies microrna that target nox2 and improve function after acute myocardial infarction. Am J Physiol Heart Circ Physiol 2017;312:H1002-H1012.
18 Fei L, Zhang J, Niu H, Yuan C, Ma X: Effects of rosuvastatin and mir-126 on myocardial injury induced by acute myocardial infarction in rats: Role of vascular endothelial growth factor a (vegf-a). Med Sci Monit 2016;22:2324-2334.
19 Long G, Wang F, Duan Q, Chen F, Yang S, Gong W, Wang Y, Chen C, Wang DW: Human circulating microrna-1 and microrna-126 as potential novel indicators for acute myocardial infarction. Int J Biol Sci 2012;8:811-818.
20 Chen X, Yan L, Guo Z, Chen Z, Chen Y, Li M, Huang C, Zhang X, Chen L: Adipose-derived mesenchymal stem cells promote the survival of fat grafts via crosstalk between the nrf2 and tlr4 pathways. Cell Death Dis 2016;7:e2369.
21 Cen W, Chen Z, Gu N, Hoppe R: Prevention of ami induced ventricular remodeling: Inhibitory effects of heart-protecting musk pill on il-6 and tnf-alpha. Evid Based Complement Alternat Med 2017;2017:3217395.
22 Qu Y, Zhang Q, Cai X, Li F, Ma Z, Xu M, Lu L: Exosomes derived from mir-181-5p-modified adipose-derived mesenchymal stem cells prevent liver fibrosis via autophagy activation. J Cell Mol Med 2017;21:2491-2502.
23 Zhang Y, Yu M, Dai M, Chen C, Tang Q, Jing W, Wang H, Tian W: Mir-450a-5p within rat adipose tissue exosome-like vesicles promotes adipogenic differentiation by targeting wisp2. J Cell Sci 2017;130:1158-1168.

24 Pu CM, Liu CW, Liang CJ, Yen YH, Chen SH, Jiang-Shieh YF, Chien CL, Chen YC, Chen YL: Adipose-derived stem cells protect skin flaps against ischemia/reperfusion injury via il-6 expression. J Invest Dermatol 2017;137:1353-1362.
25 Lee M, Ban JJ, Kim KY, Jeon GS, Im W, Sung JJ, Kim M: Adipose-derived stem cell exosomes alleviate pathology of amyotrophic lateral sclerosis *in vitro*. Biochem Biophys Res Commun 2016;479:434-439.
26 Suzuki E, Fujita D, Takahashi M, Oba S, Nishimatsu H: Stem cell-derived exosomes as a therapeutic tool for cardiovascular disease. World J Stem Cells 2016;8:297-305.
27 Gallet R, Dawkins J, Valle J, Simsolo E, de Couto G, Middleton R, Tseliou E, Luthringer D, Kreke M, Smith RR, Marban L, Ghaleb B, Marban E: Exosomes secreted by cardiosphere-derived cells reduce scarring, attenuate adverse remodelling, and improve function in acute and chronic porcine myocardial infarction. Eur Heart J 2017;38:201-211.
28 Esser JS, Saretzki E, Pankratz F, Engert B, Grundmann S, Bode C, Moser M, Zhou Q: Bone morphogenetic protein 4 regulates microrna mir-494 and mir-126-5p in control of endothelial cell function in angiogenesis. Thromb Haemost 2017;117:734-749.
29 Zhang J, Sun XJ, Chen J, Hu ZW, Wang L, Gu DM, Wang AP: Increasing the mir-126 expression in the peripheral blood of patients with diabetic foot ulcers treated with maggot debridement therapy. J Diabetes Complications 2017;31:241-244.
30 Tao SC, Guo SC, Li M, Ke QF, Guo YP, Zhang CQ: Chitosan wound dressings incorporating exosomes derived from microrna-126-overexpressing synovium mesenchymal stem cells provide sustained release of exosomes and heal full-thickness skin defects in a diabetic rat model. Stem Cells Transl Med 2017;6:736-747.
31 Hsu A, Chen SJ, Chang YS, Chen HC, Chu PH: Systemic approach to identify serum microrna as potential biomarkers for acute myocardial infarction. Biomed Res Int 2014;2014:418628.
32 Wang S, Aurora AB, Johnson BA, Qi X, McAnally J, Hill JA, Richardson JA, Bassel-Duby R, Olson EN: The endothelial-specific microrna mir-126 governs vascular integrity and angiogenesis. Dev Cell 2008;15:261-271.
33 Guo C, Sah JF, Beard L, Willson JK, Markowitz SD, Guda K: The noncoding rna, mir-126, suppresses the growth of neoplastic cells by targeting phosphatidylinositol 3-kinase signaling and is frequently lost in colon cancers. Genes Chromosomes Cancer 2008;47:939-946.
34 Banerjee N, Kim H, Talcott S, Mertens-Talcott S: Pomegranate polyphenolics suppressed azoxymethane-induced colorectal aberrant crypt foci and inflammation: Possible role of mir-126/vcam-1 and mir-126/pi3k/akt/mtor. Carcinogenesis 2013;34:2814-2822.
35 Angel-Morales G, Noratto G, Mertens-Talcott S: Red wine polyphenolics reduce the expression of inflammation markers in human colon-derived ccd-18co myofibroblast cells: Potential role of microrna-126 Food Funct 2012;3:745-752.
36 Hu J, Zeng L, Huang J, Wang G, Lu H: Mir-126 promotes angiogenesis and attenuates inflammation after contusion spinal cord injury in rats. Brain Res 2015;1608:191-202.
37 Wang Z, Wang L, Su X, Pu J, Jiang M, He B: Rational transplant timing and dose of mesenchymal stromal cells in patients with acute myocardial infarction: A meta-analysis of randomized controlled trials. Stem Cell Res Ther 2017;8:21.
38 Tao B, Cui M, Wang C, Ma S, Wu F, Yi F, Qin X, Liu J, Wang H, Wang Z, Ma X, Tian J, Chen Y, Wang J, Cao F: Percutaneous intramyocardial delivery of mesenchymal stem cells induces superior improvement in regional left ventricular function compared with bone marrow mononuclear cells in porcine myocardial infarcted heart. Theranostics 2015;5:196-205.
39 Dai G, Xu Q, Luo R, Gao J, Chen H, Deng Y, Li Y, Wang Y, Yuan W, Wu X: Atorvastatin treatment improves effects of implanted mesenchymal stem cells: Meta-analysis of animal models with acute myocardial infarction. BMC Cardiovasc Disord 2015;15:170.
40 Lu W, Xie Z, Tang Y, Bai L, Yao Y, Fu C, Ma G: Photoluminescent mesoporous silicon nanoparticles with siccr2 improve the effects of mesenchymal stromal cell transplantation after acute myocardial infarction. Theranostics 2015;5:1068-1082.
41 Garcia-Contreras M, Vera-Donoso CD, Hernandez-Andreu JM, Garcia-Verdugo JM, Oltra E: Therapeutic potential of human adipose-derived stem cells (adscs) from cancer patients: A pilot study. PLoS One 2014;9:e113288.